



ELSEVIER

18 December 2000

Physics Letters A 278 (2000) 88–94

PHYSICS LETTERS A

www.elsevier.nl/locate/pla

# The energy spectrum of parabolic quantum dots

Chun-Chin Yang<sup>a,\*</sup>, Yung-Sheng Huang<sup>b</sup><sup>a</sup> Department of Physics, National Changhua University of Education, Changhua 500, Taiwan<sup>b</sup> Department of Electro-Physics, National Chiao-Tung University, Hsinchu 300, Taiwan

Received 25 May 2000; received in revised form 2 November 2000; accepted 7 November 2000

Communicated by A. Lagendijk

## Abstract

We calculate the energy spectrum of hydrogen impurity located in the center of parabolic quantum dot. The energy levels under this model differ from the previous results for the case of spherical quantum dot. The degeneracy of the energy levels is quite different as well. However, compared with the spherical quantum dot, the energy plateau under this model is not obvious. © 2000 Elsevier Science B.V. All rights reserved.

PACS: 73.20.Dx; 03.65.Ge; 85.30.Vw

Keywords: Quantum dot; Parabolic coordinates

## 1. Introduction

Due to the high progress in scientific technology in the past few years, people can now make “artificial atom” or “quantum dots”, as they are called [1,2]. Since the scale of these nano structures has approached to the size of an atom, physicists are trying to enclose the quantum mechanism behind. The simplest model is an hydrogen atom in the center of a spherical cavity with a discontinuous potential to simulate the quantum dot. Many results on this model have been reported [3–5]. Huang et al. first solved the relativistic version of the model [6]. From application point of view, the characteristic of level crossing of a quantum dot provides a new method for controlling level stability [7–9]. However, the spherical cavity is still not good enough for a real quantum dot. In this Letter, another model, a parabolic quantum dot, is

presented. The eigenenergies and wavefunctions are also obtained from hydrogen impurity. Some novel properties under this model are found and compared with those of a spherical dot.

## 2. Theory

To study the interesting properties of parabolic quantum dot, we use parabolic coordinate system. First we transform the coordinate system from spherical coordinates  $(r, \theta, \varphi)$  to parabolic coordinates  $(\xi, \eta, \varphi)$  [10]. Taking the coordinate system as equal-potential surface in the boundary, we can simulate a parabolic cavity. The geometry of the parabolic cavity can be defined through the following relations:

$$\xi = r + z = R_0, \quad (2.1)$$

$$\eta = r - z = R_0, \quad (2.2)$$

where  $R_0$  is the size of the parabolic cavity, or the radius of a parabolic quantum dot in the  $x$ – $y$  plane at

\* Corresponding author. Fax: 886-4-721153.

E-mail address: phyan@cc.ncue.edu.tw (C.-C. Yang).

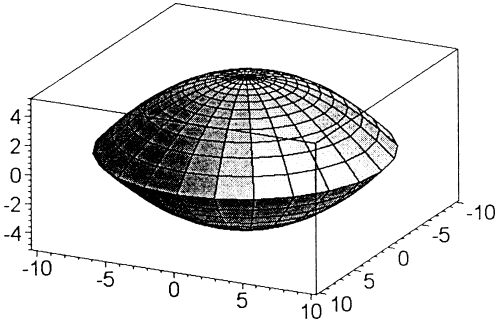


Fig. 1. The geometry of a parabolic quantum dot.

$z = 0$ . The cavity is rotationally symmetric along the  $z$ -axis as shown in Fig. 1. Let us consider a hydrogen impurity located in the center of a parabolic cavity. The Hamiltonian of a hydrogen impurity inside such a cavity is

$$H = -\frac{\hbar^2}{2\mu}\nabla^2 - \frac{Ze^2}{\varepsilon r} + V, \quad (2.3)$$

where

$$V = \begin{cases} -V_0, & \xi \leq R_0, \eta \leq R_0, \\ 0, & \text{otherwise,} \end{cases} \quad (2.4)$$

which means that the potential inside the cavity is shifted by a negative constant,  $-V_0$ , compared with the potential of a hydrogen atom. The parameters  $\mu$ ,  $\varepsilon$ , and  $Z$  are the effective mass, the electrical constant, and the core charge, respectively. We use the effective Bohr radius,  $a = \hbar^2\varepsilon/\mu e^2$ , as the unit of length, and the effective Rydberg,  $R_y^* = \mu e^4/2\hbar^2\varepsilon^2$ , as the unit of energy. For hydrogen atom,  $a$  is about 0.53 Å and  $R_y^*$  is about 13.6 eV. For a hydrogen impurity in GaAs,  $a$  is about 100 Å and  $R_y^*$  is about 5.48 meV.

Next, we deal with the Schrödinger equation by setting

$$\Psi(\xi, \eta, \varphi) = u(\xi)v(\eta)e^{im\varphi}, \quad (2.5)$$

$$Z = Z_1 + Z_2. \quad (2.6)$$

Then, let us carry out the separation. Since  $\xi$  and  $\eta$  are symmetric, we treat the differential equation satisfied by  $u(\xi)$  as follows:

$$\begin{aligned} \frac{d}{d\xi}\left(\xi\frac{du(\xi)}{d\xi}\right) + \left(\frac{1}{2}\xi(E-V) - \frac{m^2}{4\xi}\right)u(\xi) \\ = -Z_1u(\xi), \end{aligned} \quad (2.7)$$

where  $V$  is described in Eq. (2.4). Outside the cavity, this term  $V$  shall be dropped. The solutions of the bound states can be expressed in terms of generalized hypergeometric function as follows:

Solution regular at  $r = 0$ :

$$u_{\text{in}}(\xi) \sim e^{-\beta\xi}\xi_1^{|m|/2}F_1(-n_1, |m|+1, 2\beta\xi), \quad (2.8)$$

where

$$\beta \equiv \sqrt{-(E+V_0)}/2, \quad (2.9)$$

$$n_1 \equiv \frac{Z_1}{2\beta} - \frac{1}{2}(|m|+1). \quad (2.10)$$

Solutions regular at  $r = \infty$ :

$$u_{\text{out}}(\xi) \sim e^{-\beta'\xi}\xi_2^{n'_1-|m|/2}F_0\left(-n'_1, |m|-n'_1, \frac{-1}{2\beta'\xi}\right), \quad (2.11)$$

where

$$\beta' \equiv \sqrt{-\frac{E}{2}}, \quad (2.12)$$

$$n'_1 \equiv \frac{Z_1}{2\beta'} + \frac{1}{2}(|m|-1). \quad (2.13)$$

Eqs. (2.7)–(2.13) may be applied to  $v(\eta)$  if the parameter  $Z_1$  is replaced by  $Z_2$  and the variable  $\xi$  is replaced by  $\eta$ , respectively.

For finite confining potential  $V_0$ , it is necessary that both the wavefunction and its first derivatives be continuous at the boundary  $R_0$ . With these boundary conditions and the requirement shown in Eq. (2.6), both  $u(\xi)$  and  $v(\eta)$  can be found. The wavefunctions can then be obtained from Eq. (2.5).

Assuming  $\hat{O}$  is an observable operator, its expectation value is given by

$$\langle \hat{O} \rangle = \frac{\int_0^\infty d\xi \int_0^\infty d\eta \int_0^{2\pi} d\phi \hat{O} |\psi|^2(\xi + \eta)}{\int_0^\infty d\xi \int_0^\infty d\eta \int_0^{2\pi} d\phi |\psi|^2(\xi + \eta)}. \quad (2.14)$$

When  $R_0 = 0$  or  $\infty$ , we find that the expectation values of  $\xi$ ,  $\eta$ ,  $r$  and  $z$  can be expressed as analytic close form, which are given as follows:

$$\langle \xi \rangle = \left( n^2 z_1 (z_1 + 2) + \frac{1-m^2}{4} \right) / Z, \quad (2.15)$$

$$\langle \eta \rangle = \left( n^2 z_2 (z_2 + 2) + \frac{1-m^2}{4} \right) / Z, \quad (2.16)$$

$$\langle r \rangle = \left( n^2 \left( \frac{3}{2} - z_1 z_2 \right) + \frac{1-m^2}{4} \right) / Z, \quad (2.17)$$

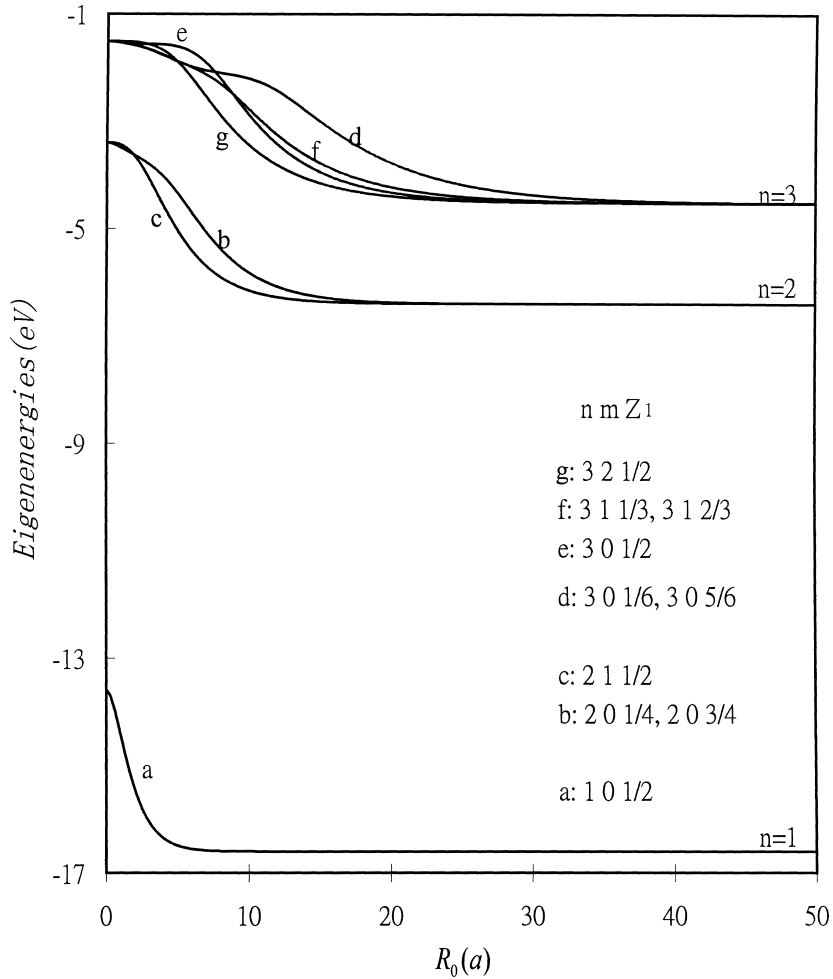


Fig. 2. The eigenenergies of parabolic quantum dot in low excited states  $n = 1, 2, 3$  as functions of  $R_0$ . Compared with spherical quantum dot, the energy plateau is not very clear.

$$\langle z \rangle = \left( \frac{3}{2} n^2 (z_1 - z_2) \right) / Z, \tag{2.18}$$

where  $z_j = Z_j / Z$ .

### 3. Results and discussion

In our calculation,  $V_0$  is chosen to be 3 eV and the nuclear charge  $Z$  is equal to 1. Different values of  $V_0$  and  $Z$  can be used when needed. From Fig. 2, we find that

- (1) At  $R_0 = 0$  and  $\infty$ , it has correct limit. When dot size is extremely small, the eigenenergy  $E$  of the impurity approaches to the corresponding energy of a free-space hydrogen:  $E \cong -R_y^*/n^2$ . When the radius of the dot is large enough, the eigenenergies approach to the values which are equal to the confining potential plus the corresponding energy of a free-space hydrogen:  $E \cong -(Z^2 R_y^*/n^2 + V_0)$ .
- (2) The model shows level crossing for  $n = 2$  and  $n = 3$  states, just like spherical quantum dot does. But the energy plateau of this model is not so clear as the one in spherical quantum dot. The

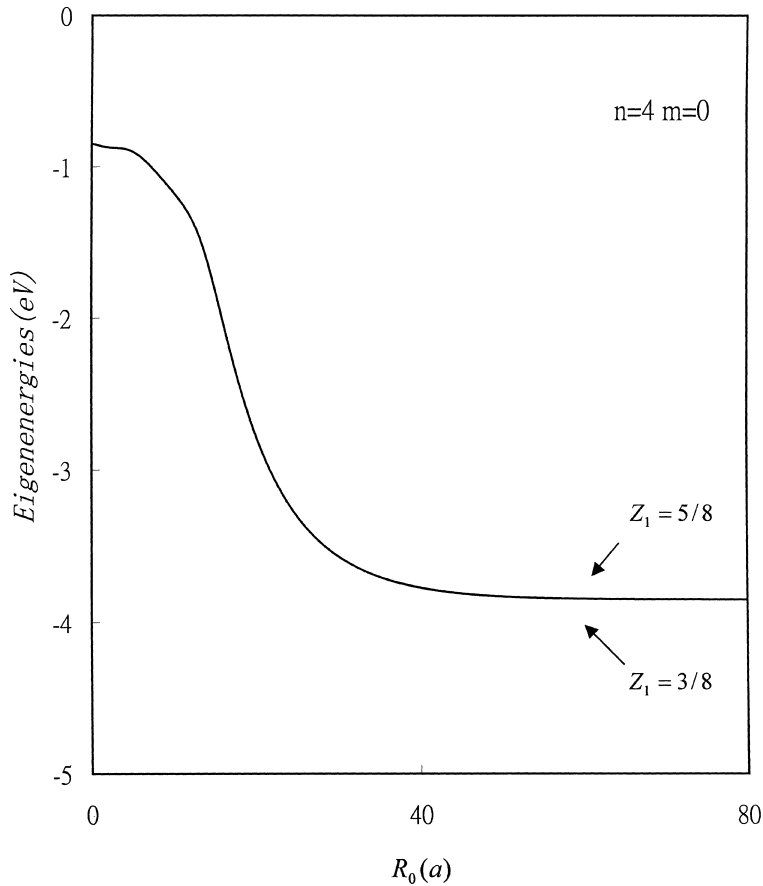


Fig. 3. Eigenenergies as functions of  $R_0$  for the state  $n = 4$ ,  $m = 0$  and  $Z_1 = 3/8$  and  $5/8$ , respectively. The two curves overlap. It follows that  $Z_1 = 3/8$  and  $5/8$  are degenerate states in parabolic quantum dot.

results for principal quantum number  $n = 1, 2, 3$  are shown in Fig. 2 for demonstration.

For each  $Z_1 \neq 1/2$  state with fixed  $n$  and  $m$ , there exists a degenerate state with  $Z'_1 = 1 - Z_1$ . The degeneracy of this pair can not be destroyed by the size of the dot. For example, the states  $n = 4$ ,  $m = 0$  with  $Z_1 = 3/8$  and  $5/8$ , respectively, are degenerate. This can be seen from Fig. 3, where we get the same energy spectrum when plotting the eigenenergies as functions of  $R_0$  for  $Z_1 = 3/8$  and  $5/8$ .

At  $R_0 = 0$  and  $\infty$ , the eigenenergies are in  $n^2$ -degeneracy as the degeneracy of a free-space hydrogen atom. Between these two extreme situations, the  $n^2$ -degeneracy disappears. For any specific  $n$ , it is found that the number of the maximum splitting levels is

$[(n + 1)/2]^2$  if  $n$  is odd, and  $n(n + 2)/4$  if  $n$  is even. This phenomenon is very different from the spherical quantum dot [5], where the number of the maximum splitting levels is  $n$  for any principal quantum number  $n$ . More detailed results are listed in Table 1.

In Fig. 4, we plot  $Z_1$  as functions of  $R_0$ . We can see that even in the region  $R_0 < 40$  Bohr radius, where the oscillation occurs,  $Z_1$  are always complementary to each other, namely, their summation is equal to 1. Moreover, they correspond to the same eigenenergy. Therefore, we expect the same behavior in another group of degenerate states  $Z_1 = 1/8$  and  $7/8$ .

In Fig. 5, we present expectation values of  $\xi$ ,  $\eta$ ,  $r$  and  $z$  as functions of the dot size for the pair states of  $n = 4$ ,  $m = 0$ ,  $Z_1 = 3/8$  ( $5/8$ ). When the dot size is

Table 1

Quantum number and degeneracy of free-space hydrogen are shown in the first four columns. The last column is revealed the maximum energy levels splitting for each  $n$  of the parabolic quantum dot

$n$	$m$	$Z_1$	Degeneracy	Max. splitting	
1	0	1/2	1	1	
2	0	1/4 3/4	2		
	$\pm 1$	1/2			
3	0	1/6 1/2 5/6	4		
	$\pm 1$	1/3 2/3			
	$\pm 2$	1/2			
4	0	1/8 3/8 5/8 7/8	16	6	
	$\pm 1$	1/4 1/2 3/4			
	$\pm 2$	3/8 5/8			
	$\pm 3$	1/2			
5	0	1/10 3/10 1/2 7/10 9/10	25	9	
	$\pm 1$	1/5 2/5 3/5 4/5			
	$\pm 2$	3/10 1/2 7/10			
	$\pm 3$	2/5 3/5			
	$\pm 4$	1/2			
6	0	1/12 1/4 5/12 7/12 3/4 11/12	36	12	
	$\pm 1$	1/6 1/3 1/2 2/3 5/6			
	$\pm 2$	1/4 5/12 7/12 3/4			
	$\pm 3$	1/3 1/2 2/3			
	$\pm 4$	5/12 7/12			
	$\pm 5$	1/2			
any $n$	0	$\frac{1}{2n} \frac{3}{2n} \frac{5}{2n} \dots \frac{(2n-1)}{2n}$	$n^2$	$\left(\frac{n+1}{2}\right)^2$ odd $n$	
	$\pm 1$	$\frac{2}{2n} \frac{4}{2n} \frac{6}{2n} \dots \frac{(2n-2)}{2n}$			$\frac{n(n+2)}{4}$ even $n$
	$\vdots$	$\vdots$			
	$\pm(n-1)$	$\frac{1}{2}$			

extremely small or extremely large, all the expectation values satisfy Eqs. (2.15)–(2.18). We notice that the  $\xi$ -expectation value for  $Z_1 = 3/8$  is consistent with the  $\eta$ -expectation value for  $Z_1 = 5/8$ , independent of

the dot size. Similarly,  $\langle \xi \rangle_{5/8}$  is equal to  $\langle \eta \rangle_{3/8}$ . We also notice that  $\langle r \rangle_{3/8} = \langle r \rangle_{5/8}$  for any dot size. The  $z$ -expectation values of this pair are symmetric as a function of dot size, with extreme point at  $R_0 \cong 23a$ .

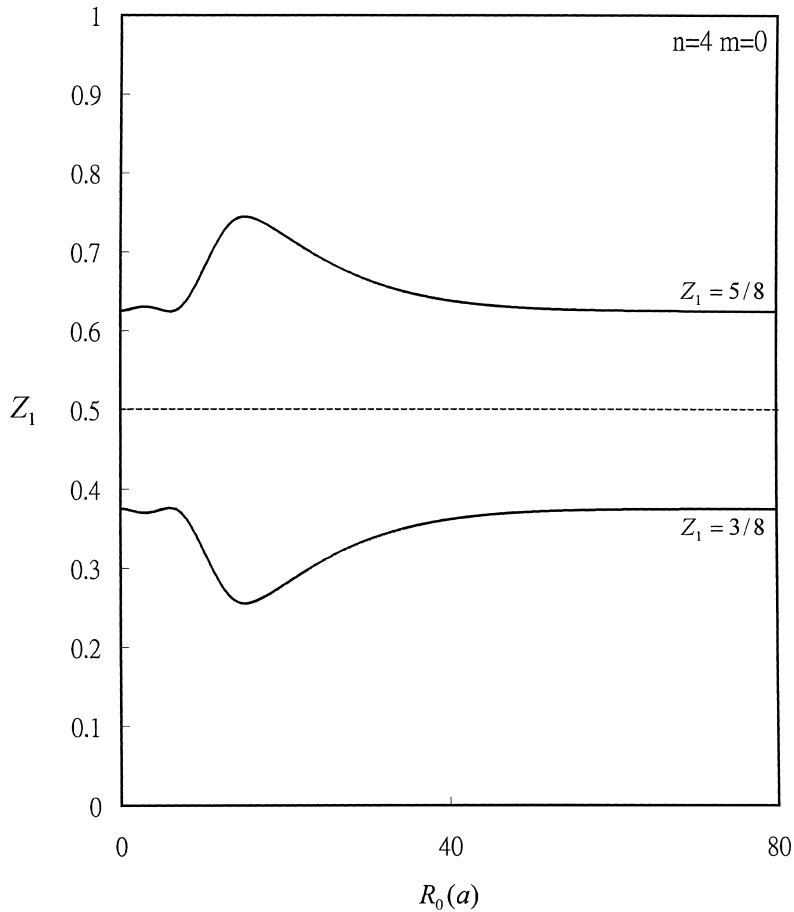


Fig. 4.  $Z_1$  as functions of  $R_0$  for the state  $n = 4$ ,  $m = 0$ ,  $Z_1 = 3/8$  and  $5/8$  with the same energy. It is found that the two quantum number of this degenerate state is complementary to each other.

#### 4. Conclusion

This Letter contains new results on the quantum dot. We apply the parabolic coordinate to study the characteristics of the hydrogen impurity in a parabolic cavity, which has never been studied before. We solve Schrödinger equation to obtain the system wavefunctions, eigenvalues, and their degeneracy analytically. We find that the parabolic quantum dot has several features different from those of a spherical quantum dot. Since many researchers are now working on the electronic states in quantum dot, these results would be helpful for people to understand quantum dot and

manufacture artificial atom. Furthermore, in the parabolic coordinates, one can also study the phenomena of a quantum dot exposed to a constant electric field.

#### Acknowledgement

The authors would like to thank Professor S.S. Liaw for providing the idea on this study. This work was supported by the National Science Council of Republic of China under Grant No. NSC 89-2112-M-018-013.

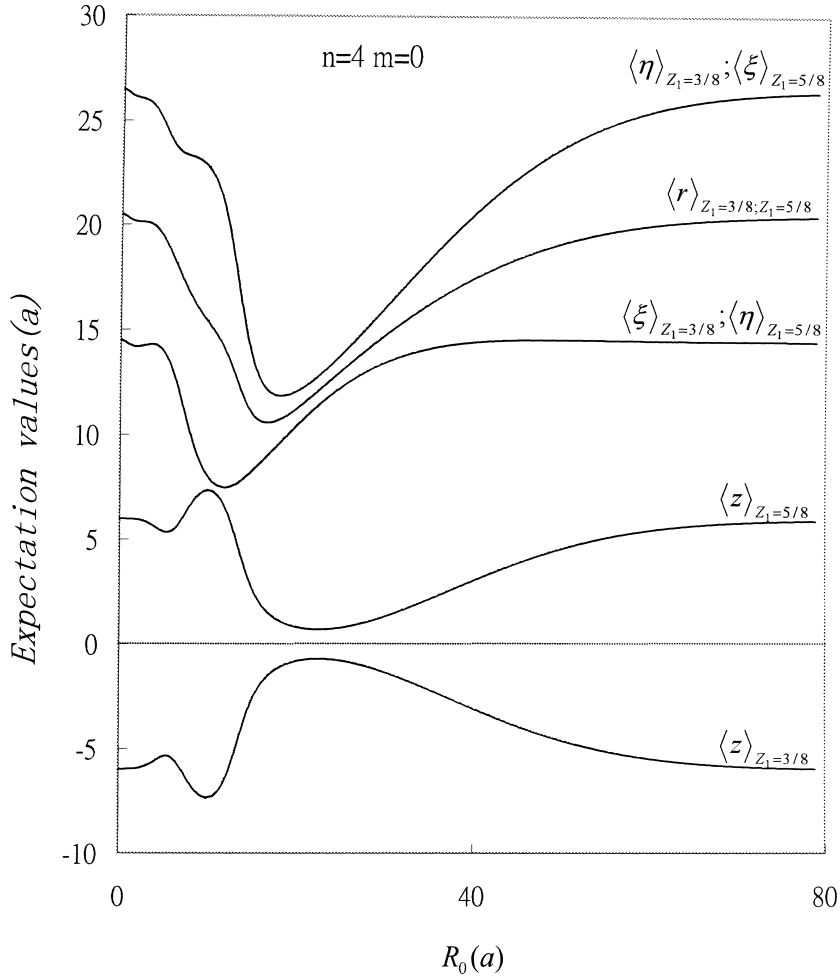


Fig. 5. The electron probability for different space variables  $\langle \eta \rangle$ ,  $\langle \xi \rangle$ ,  $\langle r \rangle$ ,  $\langle z \rangle$  as functions of  $R_0$  for the state  $n = 4$ ,  $m = 0$ ,  $Z_1 = 3/8$  and  $5/8$ .

## References

- [1] M.A. Kastner, Phys. Today 24 (1993).
- [2] M.A. Reed, Sci. Am. 98 (1993).
- [3] J.L. Zhu, J. Wu, R.T. Fu, H. Chen, Y. Kawazoe, Phys. Rev. B 55 (1997) 1673.
- [4] D.S. Chu, C.M. Hsiao, W.N. Mei, Phys. Rev. B 46 (1992) 3839.
- [5] C.C. Yang, L.C. Liu, S.H. Chang, Phys. Rev. B 58 (1998) 1954.
- [6] Y.S. Huang, C.C. Yang, S.S. Liaw, Phys. Rev. A 60 (1999) 85.
- [7] Y.S. Huang, S.S. Liaw, Mod. Phys. Lett. B 13 (1999) 977.
- [8] J.P. Connerade, V.K. Dolmatov, J. Phys. B 31 (1998) 3557.
- [9] J.P. Connerade, V.K. Dolmatov, P.A. Lakshmi, S.T. Manson, J. Phys. B 32 (1999) L239.
- [10] H.A. Bethe, E.E. Salpeter, Quantum Mechanics of One- and Two-Electron Atoms, Plenum New, York, 1957.